Fig. S1

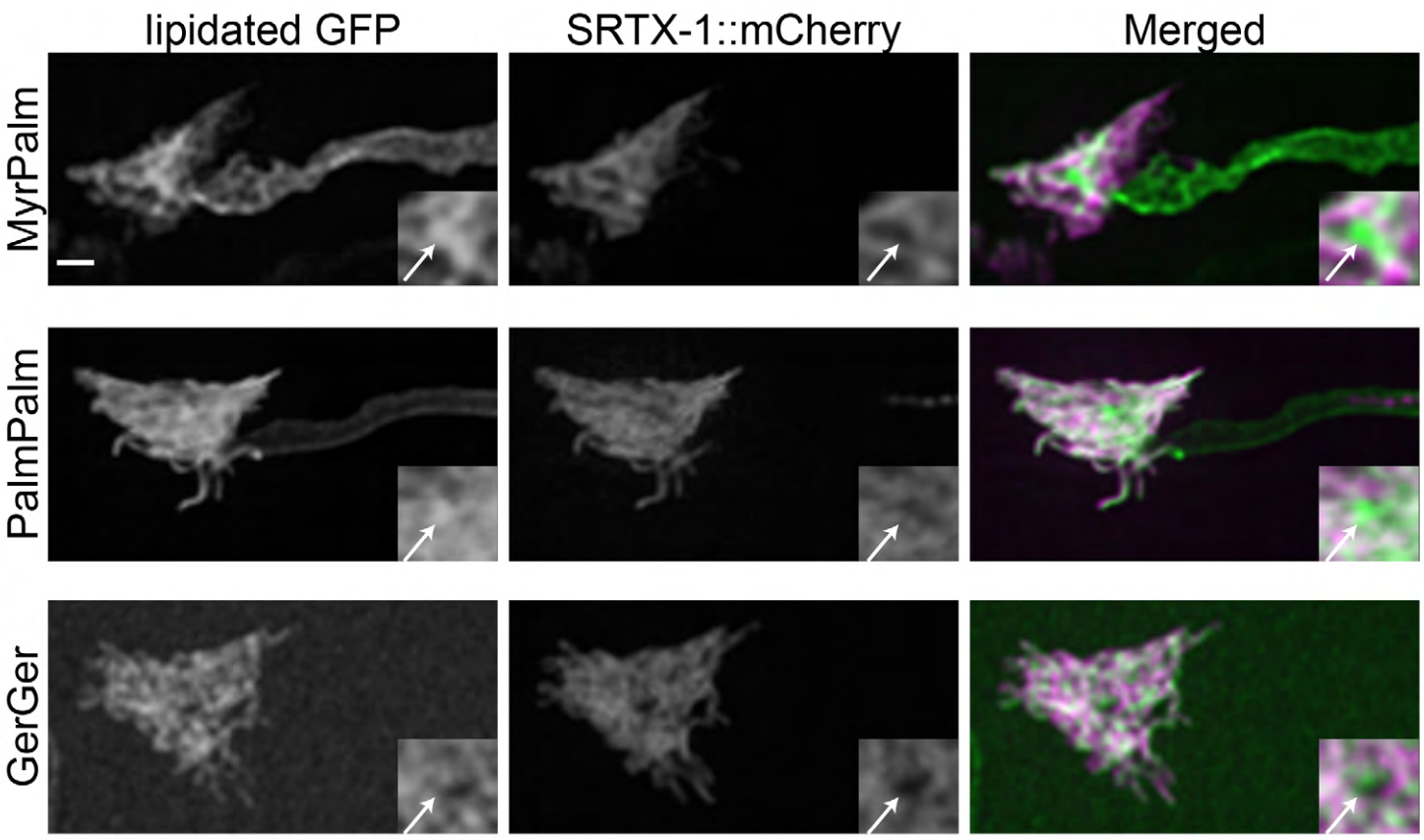
lipidated GFP
SRTX-1::mCherry
Merged
MyrPalm
PalmPalm
GerGer

Fig. S2

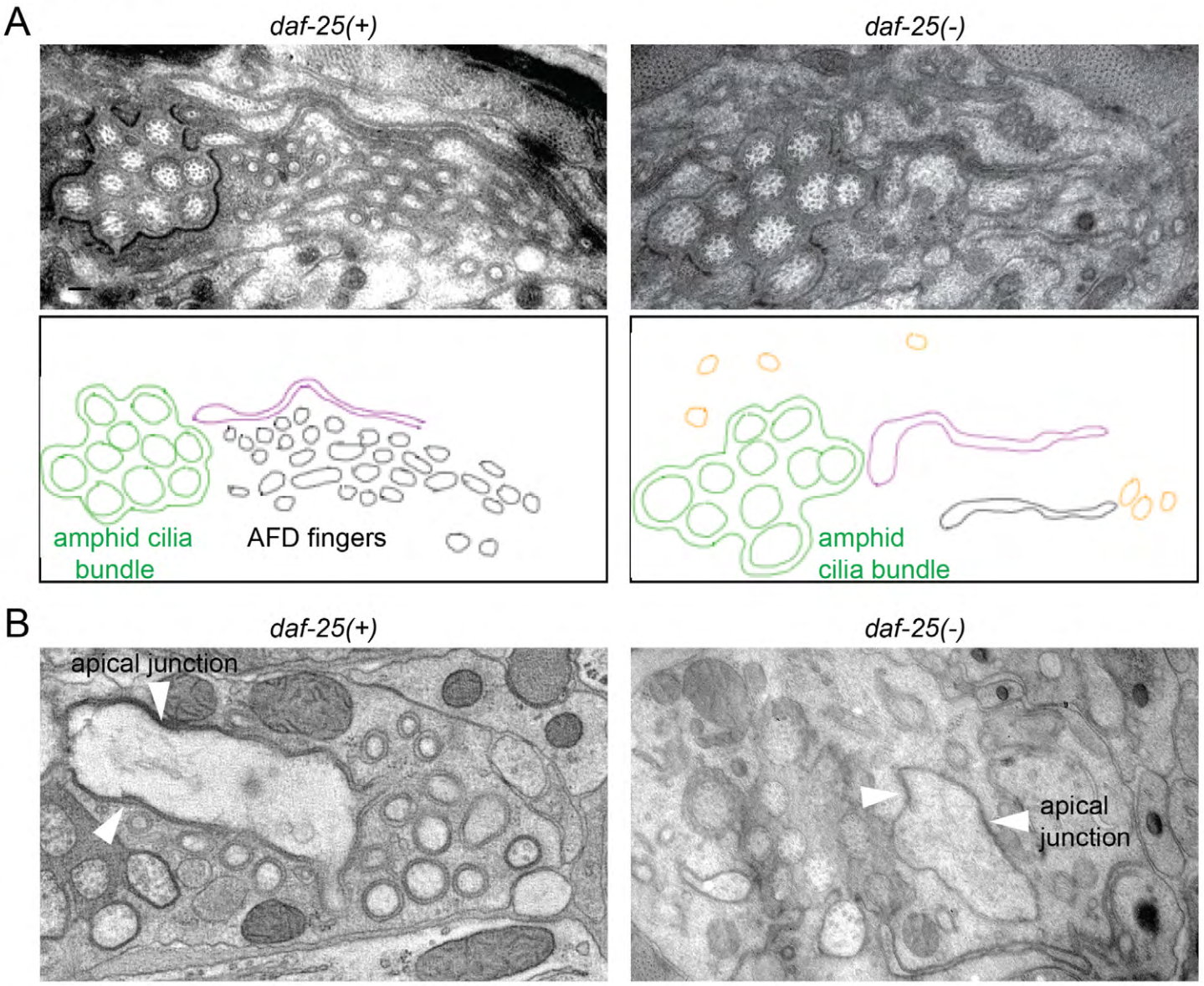
A
daf-25(+)
daf-25(-)
amphid cilia bundle
AFD fingers
amphid cilia bundle
B
daf-25(+)
daf-25(-)
apical junction
apical junction

Fig. S3

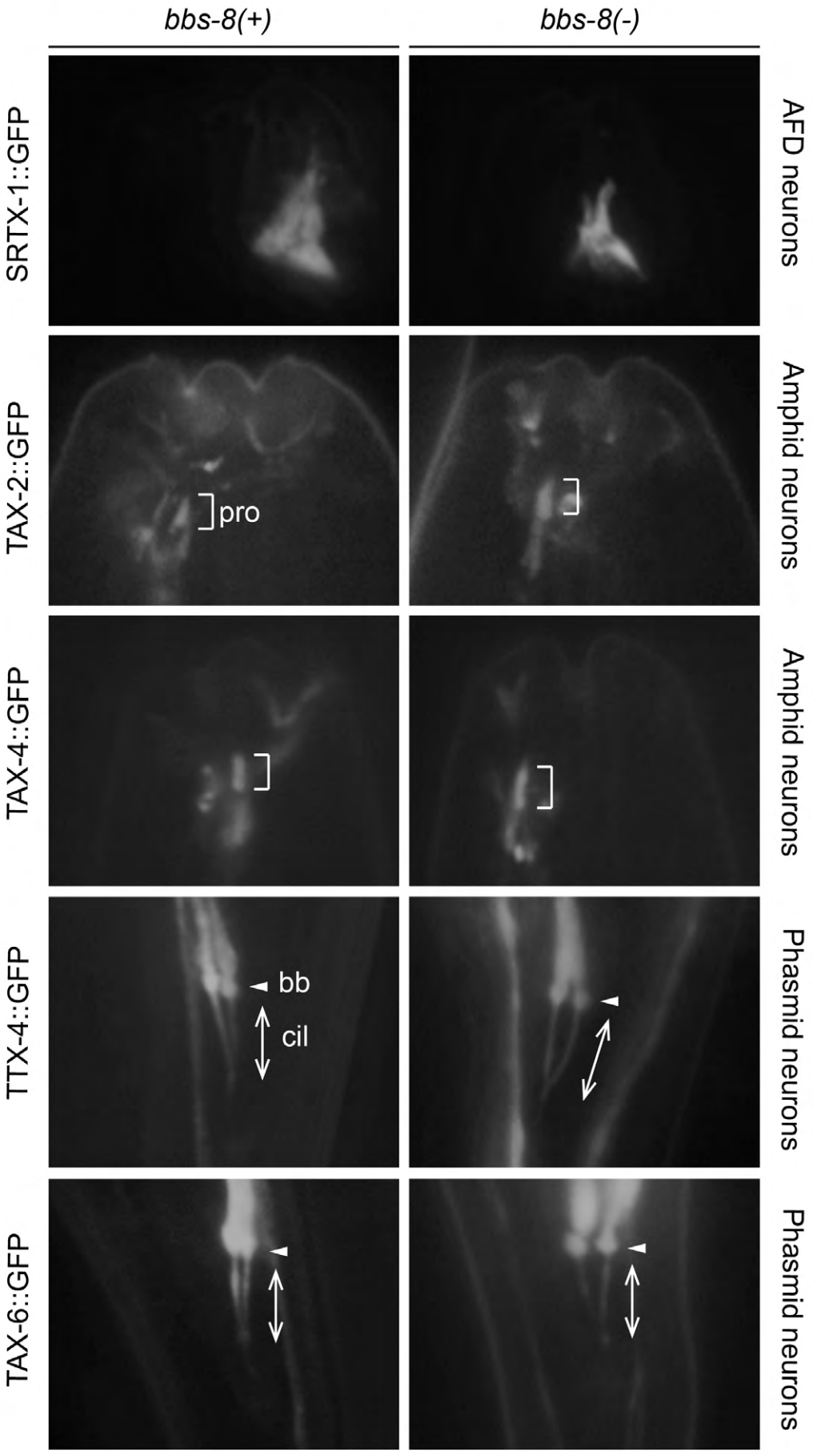
bbs-8(+)
bbs-8(-)
SRTX-1::GFP
AFD neurons
TAX-2::GFP
pro
Amphid neurons
TAX-4::GFP
Amphid neurons
TTX-4::GFP
bb
cil
Phasmid neurons
TAX-6::GFP
Phasmid neurons

Fig. S4

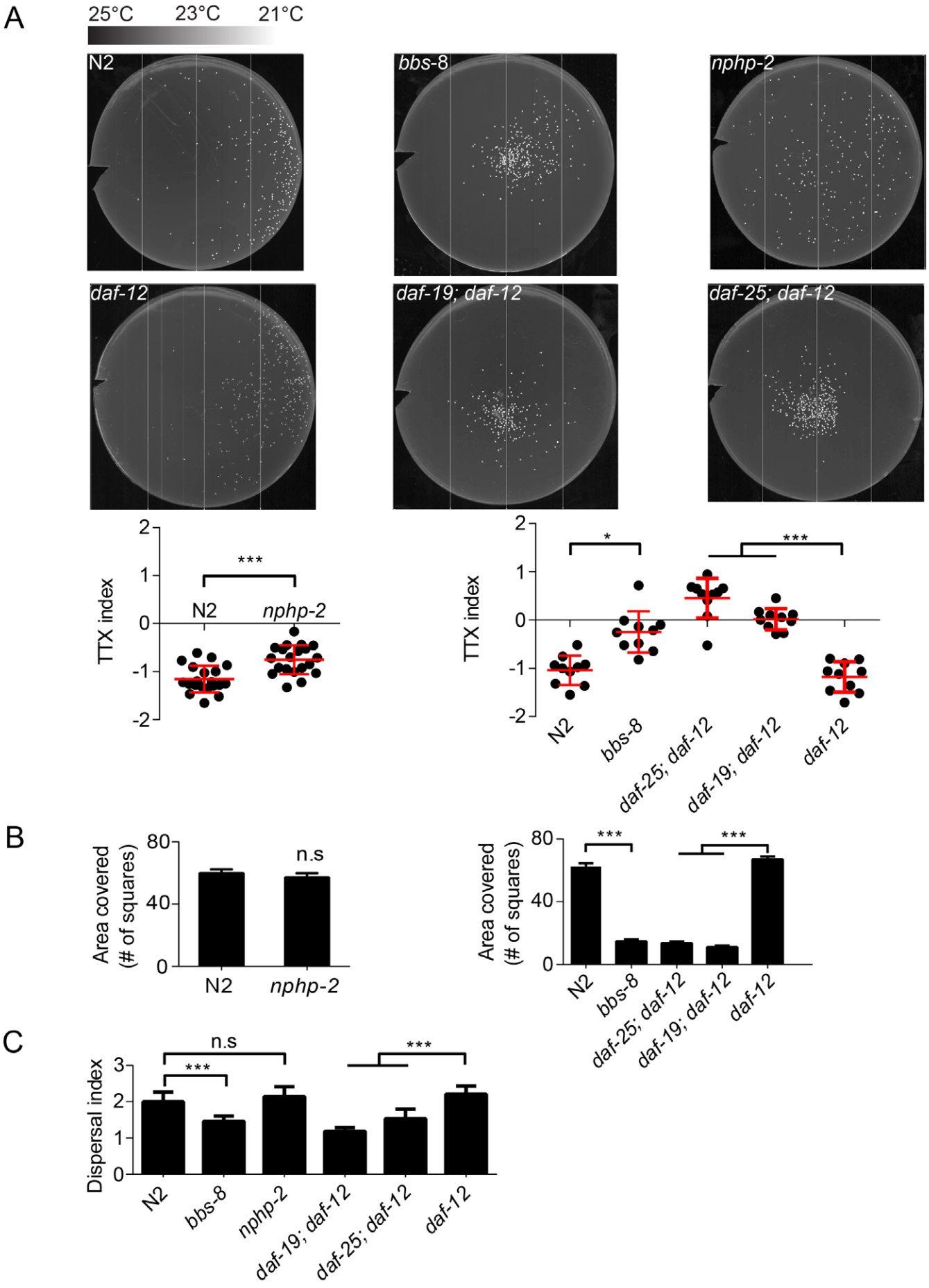
A
25°C
23°C
21°C
N2
bbs-8
nphp-2
daf-12
daf-19; daf-12
daf-25; daf-12
TTX index
***
N2
nphp-2
*
***
bbs-8
daf-25; daf-12
daf-19; daf-12
daf-12
B
Area covered (# of squares)
n.s
N2
nphp-2
C
Dispersal index
n.s
***
***
***
N2
bbs-8
nphp-2
daf-19; daf-12
daf-25; daf-12
daf-12

Fig. S1. Different lipidated GFP constructs localize to different membrane compartments in the AFD neurons.

Acylated GFP (PalmMyr and MyrMyr GFP) is present throughout the dendritic, finger, and possibly ciliary membranes, whereas prenylated GFP (GerGer GFP) is localized specifically to the finger membrane (marked with SRTX-1). Arrows indicate the position of the cilium, as inferred by the lack of SRTX-1 signal. Scale bar is 1 μm.

Fig. S2. *daf-25* mutant worms have abnormal finger formation.

One-day adult worms were fixed in 2.5% glutaldehyde, 1% paraformaldehyde, refixed in 1% osmium tetroxide, and then stained with 1% uranium acetate. After dehydration, samples were embedded in Embed-812 resin medium mixture (EMS) and electron micrographs were collected with a Philips CM10 microscope. (A) About 30 fingers (illustrated in black) can be seen in wild-type worms (n=2), whereas in *daf-25* worms they cannot be distinguished as easily (n=3). Double-membrane structures seen in mutant worms (orange) could be part of AWA cilia, due to the presence of microtubules in the middle, and their location relative to the amphid bundle (green) and the AWC wing structure (magenta). Scale bar is 200 nm. (B) Apical junctions (white arrowheads) at the amphid channel appear to be normal in *daf-25* animals.

Fig. S3. cGMP signaling proteins SRTX-1, TAX-2, TAX-4, TTX-4, and TAX-6 localize normally in the *bbs-8* mutant.

Since the AFD cilia are too short for us to confidently score the phenotype in wild-type and mutant worms, our localization data are based on the patterns seen in the amphid cilia for TAX-2 and TAX-4, and in the phasmid cilia for TTX-4 and TAX-6 (the two latter proteins are also present in many non-neuronal cells in the head, obscuring the amphid localization). 'pro' (brackets) indicates ciliary proximal region; 'cil' (double-headed arrows), cilia; 'bb' (arrowheads), basal body.

Fig. S4. Ciliary mutants have defective thermotaxis and locomotory behaviors.

(A) Ciliary mutant worms show defective behavior when tested in a thermotaxis assay. Thermotaxis plates were made with Ttx medium (Mori and Ohshima, 1995). About 100 to 300 one-day-old adults raised at 20°C were collected and washed twice with M9 media, and then were placed in the 23°C zone (in the middle) of thermotaxis plates without food on a linear temperature gradient (0.5°C/cm) as described in Tan et al. (2007). After 30 minutes, the plates were scanned and the resulting images were analyzed as follows: The plate was divided longitudinally into 4 equal parts, each corresponding roughly to a one-degree zone. The number of worms in each part was counted and a thermotaxis index was calculated as $(2a+b-c-2d)/(a+b+c+d)$, with a being the number of worms in the hottest zone, d the coldest. Experiments were repeated at least 10 times. Student's t-test or one-way ANOVA with Bonferroni *post hoc* correction was used to test for significant differences in all behavioral assays. Representative thermotaxis plates show the distribution on a linear temperature gradient of different ciliary mutant worms raised at 20°C. Worm positions are highlighted by white dots. The graph represents the thermotaxis index of ciliary mutants. Each data point is from an independent experiment, n≥10. Red bars indicate means ± SD. *** indicates significant difference at $p<0.001$; *, $p<0.05$.

(B) In the presence of food, *nphp-2* worms show normal locomotion, but *bbs-8*, *daf-25*, and *daf-19* mutants have reduced locomotion. A single, well-fed one-day-old adult was put on a 6-cm plate (with a thin lawn of OP50 bacteria covering most of the plate) and was allowed to move freely for 18-20 hours. The extent of locomotion was analyzed by counting the number of 5x5mm squares the worm travelled through. Each strain was

analyzed at least 3 times, with 10 worms used each time. The bar graph represents the mean area covered ± SEM from 3 independent experiments of 10 worms each. ‘n.s’ indicates no significant difference, *** indicates significant difference at $p<0.001$.

(C) In the absence of food, *nphp-2* worms show normal dispersal behavior, but *bbs-8*, *daf-25*, and *daf-19* mutants have reduced dispersal. Worms were prepared as in thermotaxis assay and put in the center of a Ttx plate without temperature gradient. After 30 minutes, the plates were scanned and the resulting images were analyzed as follows: The plate was divided into 4 concentric circles, the number of worms in each part was counted and a dispersal index was calculated as $(a+2b+3c+4d)/(a+b+c+d)$, with a being the number of worms in the innermost circle, d the outermost. The data from 3 repeats were used to test for significance. The bar graph represents the mean area covered ± SD from 3 independent experiments. ‘n.s’ indicates no significant difference; ***, significant difference at $p<0.001$.